Are surface water characteristics efficient to locate hyporheic biodiversity hotspots ?

Pierre Marmonier, Michel Creuzé Des Châtelliers, Olivier Radakovitch, Marie-José Dole-Olivier, A. Mayer, H. Chapuis, D. Graillot, J. Re-Bahuaud, A. Johannet, L. Cadilhac

▶ **To cite this version:**

Pierre Marmonier, Michel Creuzé Des Châtelliers, Olivier Radakovitch, Marie-José Dole-Olivier, A. Mayer, et al.. Are surface water characteristics efficient to locate hyporheic biodiversity hotspots ?. Science of the Total Environment, 2020, 738, pp.40-52. 10.1016/j.scitotenv.2020.139930 . hal-02867837

HAL Id: hal-02867837

https://imt-mines-ales.hal.science/hal-02867837v1

Submitted on 15 Jun 2020

HAL is a multi-disciplinary open access archive for the deposit and dissemination of scientific research documents, whether they are published or not. The documents may come from teaching and research institutions in France or abroad, or from public or private research centers.

L'archive ouverte pluridisciplinaire **HAL**, est destinée au dépôt et à la diffusion de documents scientifiques de niveau recherche, publiés ou non, émanant des établissements d'enseignement et de recherche français ou étrangers, des laboratoires publics ou privés.

Distributed under a Creative Commons Attribution - NonCommercial - NoDerivatives 4.0 International License

Are surface water characteristics efficient to locate hyporheic biodiversity hotspots?

Marmonier P.[1], Creuzé des Châtelliers M. [1], Dole-Olivier M.J.[1], Radakovitch O.[2,3], Mayer A.[4], Chapuis H.[5], Graillot D.[5], Re-Bahuaud J.[6], Johannet A.[6], Cadilhac L.[7]

[1]Univ. Lyon, Université Claude Bernard Lyon 1, CNRS, ENTPE, UMR 5023 LEHNA, 43 boulevard du 11 Novembre 1918, 69622 VILLEURBANNE, France

[2]Aix Marseille Univ, CNRS, IRD, INRA, Coll France, CEREGE, AIX-EN-PROVENCE, France

[3]Present address : Institut de Radioprotection et de Sûreté Nucléaire (IRSN), PSE-SRTE-LRTA, CADARACHE, France

[4]Université d'Avignon – EMMAH, UFR-ip Sciences, Technologies, Santé - Campus Jean-Henri Fabre, 301 rue Baruch de Spinoza, BP 21239, 84916 AVIGNON Cedex 9, France

[5]École Nationale des Mines de Saint-Étienne, UMR-CNRS 5600 EVS, 158 cours Fauriel, 42023 SAINT-ÉTIENNE, France

[6]IMT Mines Alès, Université de Montpellier, 6 avenue de Clavières, 30319 ALÈS, France

[7]Agence de l'Eau Rhône Méditerranée et Corse, 2 allée de Lodz, 69007 LYON, France

Abstract.

Location of river-groundwater exchange zones and biodiversity hotspot is essential for a river management plan, especially for Mediterranean karstic rivers. This location is often difficult and time-consuming when long river sectors are considered. We studied a 13 km-long sector of the Cèze River (Southern France) located in a karstic canyon. We compared five indicators of river-groundwater exchanges: longitudinal profiles of temperature, electrical conductivity and ^{222}Rn concentrations in the surface water of the river, chemical characteristics of the hyporheic water and hyporheic biodiversity. Upwelling zones occurred downstream of geomorphological heterogeneities (here at the tail of gravel bars). Surface water chemistry, especially electrical conductivity and ^{222}Rn concentrations, clearly traces large scale gaining sections, which were not associated to valley narrowing but with lateral springs, suggesting a crucial role of the geological structuration of the karstic plateau of Méjanne-le-Clap. Hyporheic water chemistry fits with the large-scale hydrological pattern, but with a high variability corresponding to local heterogeneities. The stygobite fauna (obligate groundwater organisms) and benthic EPTC (Ephemeroptera, Plecoptera, Trichoptera and Coleoptera) occurred preferentially in the gaining sections fed by groundwater, likely because of oligotrophic water and cooler temperature. The spatial distribution of river-groundwater exchange zone and hyporheic biodiversity may be thus predicted using changes in surface water chemistry, especially for electrical conductivity and ^{222}Rn concentrations.

Key words.

Macro-invertebrates, stygobite, groundwater, karstic aquifer, ^{222}Rn

1-Introduction

The relationship between a river and the surrounding groundwater may vary in space and time (Winter, 1995; Sophocleous, 2002). None or very low vertical exchanges of water are observed in rivers flowing over an impermeable substratum or when it is perched above an unsaturated zone (cases a, b, e in Malard et al., 2002). In contrast, important exchanges occur when the river is in contact with a porous aquifer containing a well-developed groundwater system (case c in Malard et al., 2002). In this situation, water exchange can occur from the river to the groundwater or reversely from the aquifer to the surface system (Schaller & Fan, 2009). These exchanges vary in time, according to season or more generally to the relative level of water in the river and the aquifer (Baxter et al., 2003). The drainage of groundwater by a river generally occurs during low-water period when water levels in the river are lower than in the aquifer (Rouch, 1992). The inflow of groundwater inside a river affects surface-water characteristic (Ward et al., 1999; Hayashi et al., 2012), for example, modifying of the thermic regime (Wawrzyniak et al., 2016) or solute concentrations (Ca, K... Grasby el al., 1999; Cook, 2013). Nutrient contents are also partly controlled by groundwater inputs: organic carbon (Ford & Naiman, 1989), nitrate (Deutsch et al., 2006) or silica (Ward et al., 1999).

The inputs of groundwater influence the benthic and hyporheic biological processes, because groundwater nutrient loads stimulate biofilm biomass and activity (Claret & Fontvieille, 1997) and also aquatic invertebrates. For example, Hunt et al. (2010) showed that abundances of benthic invertebrate increased by 35% in groundwater-fed areas compared to surface water fed zones. In the same way, Gray et al. (2010) found more diverse invertebrate communities in groundwater-fed springs than in nearby stream (two times less) or in the main river (four times less). Similarly, hyporheic biodiversity is mainly controlled by river-groundwater exchanges (Dole-Olivier & Marmonier, 1992). When sediment interstices are fed by surface water well oxygenated and rich in labile organic matter (i.e. downwelling zones) the benthic fraction of the hyporheic fauna is dominant, while in groundwater-fed areas with low dissolved oxygen, high oligotrophy and thermic stability (i.e. upwelling zones), the stygobites are dominant in the assemblages (Dole-Olivier & Marmonier, 1992; Brunke & Gonser, 1999). Thus, these downwelling/upwelling successions play a crucial role in the functioning of river sediments and must be taken into account for the location of biodiversity hotspots (Dole-Olivier, 1998) and more generally for river management (Marmonier et al., 2012).

The integration of river-groundwater exchanges in a river management plan is limited by the difficulty to localise these interaction zones at a pluri-kilometer scale of 10 or 20 km (Graillot et al., 2014; Dole-Olivier et al., 2019). On one hand, surface water chemistry is not adequate to detect exchanges in large-scale losing sections making them hard to localise (Dole-Olivier et al., 2019). On the other hand,

in large-scale gaining sections, the chemical changes may be hidden by local conditions (e.g. inputs of solutes linked to tributaries) or temporal cycles (e.g. effect of day-night alternation for thermic regime, Tonolla et al., 2010; Wawrzyniak et al., 2012, 2013). Despite these difficulties, general models of the spatial distribution of surface water/groundwater exchanges along a river were elaborated for alluvial valleys (e.g. Toth, 1963; Stanford & Word, 1993; Capderrey et al., 2013) combining two scales for geomorphological and geological characteristics: (1) at the scale of the geomorphological units, (e.g. gravel bars, riffles), local downwellings generally occur upstream of these morphological discontinuities, while local upwellings occur downstream (Hendricks & White, 1988; Dole-Olivier & Marmonier, 1992). (2) At the pluri-kilometer scale of the river section, the geological context becomes essential to locate losing and gaining sections. For example, an increase in the thickness of the alluvium linked to a depression in the impermeable substratum induces a massive surface water loss to the aquifer (losing sections, Toth, 1963, Malard et al., 2006; Capderrey et al., 2013). On the contrary, a reduction of the alluvial valley width related to a bedrock outcrop generally induces massive inputs of groundwater to the river (i.e. gaining sections, Doering et al., 2007; Marmonier et al., 2019). The interaction between these two scales makes the location of gaining (groundwater inputs inside the river) and losing areas (surface water infiltration toward the aquifer) difficult to predict: in a gaining section, the local upwellings are mostly fed by deep groundwater, while in a losing section upwellings, if present, are fed by hyporheic water that originates from the surface and follows a short hyporheic flowpath before returning to the river (Dole-Olivier et al., 2019, see supplementary material Fig. S1). Indicators of such patterns can be found in upstream-downstream profiles of surface water chemistry, for temperature or solute contents (Ward et al., 1999; Wawrzyniak et al., 2016). The ^{222}Rn is a radioactive tracer used to estimate the inflow of surface water to the hyporheic zone (Bourke et al., 2014) or groundwater contribution to rivers (Ellins et al., 1990; Cook et al., 2006; Guida et al., 2013) when surrounding rocks or bottom sediment are a source of ^{222}Rn (e.g. like granite in the Cockburn River, Cook et al., 2006). The potential link between ^{222}Rn and hyporheic biodiversity was never brought to attention before.

The objectives of the present study were to localise river-groundwater exchange zones at a pluri-kilometric scale (i.e. gaining and losing sections) to predict the location of hyporheic biodiversity hotspots along a 13 km long canyon of a karstic river (the Cèze River, Southern France). We combined five indicators of river-groundwater exchanges: the longitudinal profiles of surface water temperature, electrical conductivity (using upstream-downstream continuous measure), ^{222}Rn concentrations (using high-resolution field measurements), hyporheic water chemistry and hyporheic biodiversity. Downwelling zones are all fed by surface water and generally harbour a hyporheic fauna dominated by organisms living in surface water, whatever their location in a losing or a gaining section (Creuze

123 des Châtelliers & Reygrobellet, 1990). To identify hydrologic patterns (i.e. losing versus gaining
124 sections), we thus focused on upwelling zones (i.e. downstream end of gravel bars) where the
125 hyporheic water and fauna may be influenced directly by groundwater (in gaining sections) or by
126 surface water that upwells after a short flow path inside sediment (in losing sections, see Fig. S1). Four
127 hypotheses were considered:
128 - In a river with a heterogeneous watershed, such as the Cèze River (metamorphic upstream sector
129 followed by a calcareous canyon), the chemical characteristics of the surface water differ from the
130 surrounding karstic groundwater. In the same way, the temperature of a Mediterranean river and the
131 surrounding groundwater varies, especially during the warm season. We firstly hypothesised that
132 surface water chemistry is modified by groundwater inflow in gaining sections compared to losing
133 sections or no-exchange zones (**H1**, Cook, 2013). For this purpose, we used surface water temperature,
134 electrical conductivity profiles and changes in ^{222}Rn concentrations as indicators of exchanges. The
135 ^{222}Rn content was chosen because of the metamorphic origin of the river sediment inside the canyon.
136 - Assuming that groundwater-surface water exchange patterns described in alluvial rivers (Capderrey
137 et al., 2013) are similar in all types of rivers, we can hypothesise locations of exchange zones at two
138 scales. Firstly, at the scale of a gravel bar, as we sampled only at the downstream ends, we can predict
139 that all (or most) stations will consist in local upwelling zones, fed by deep groundwater (in gaining
140 sections) or by surface water after a short flow path inside the sediment (in losing sections, **H2,** Hof,
141 1963). Secondly, at the scale of the studied sector, gaining and losing sections can be predicted by the
142 geological context: the gaining sections are expected upstream of a canyon narrowing while losing
143 sections are expected in enlarged sections of the valley (**H2,** Hof, 1963).
144 - The composition of the hyporheic fauna is affected by the origin and the quality of the water (Stanley
145 & Boulton, 1993). The stygobite fauna, for example, requires a thermic stability and an oligotrophy
146 generally linked to groundwater inflows. We thus hypothesised that stygobite assemblages will be
147 more abundant and diversified in local upwelling located in gaining sections where hyporheic water is
148 of deep origin (**H3**, Dole-Olivier & Marmonier, 1992).
149 - In contrast, benthic fauna needs oxygenated water and labile organic matter brought inside the
150 sediment by surface water inflows (Dawy-Bower et al., 2006). We hypothesised that benthic
151 Ephemeroptera, Plecoptera, Trichoptera and Coleoptera (EPTC) may be more abundant in the losing
152 sections (**H4**, Brunke & Gonser, 1999).
153
154 **2-Studied site**
155 The Cèze River is a 135 km long Mediterranean river of the South-East France with a total difference
156 of level of 773 m. The spring of the Cèze River is located at 800 m a.s.l. in the metamorphic region of
157 the Cevennes (median Stephanien, dominated by Gneiss and Quartzit, Chapuis, 2017). The river flows

158 to the east, crosses the rift valley of Alès (5 km large) and enters the calcareous plateau of Méjeanne-
159 le-Clap (Barremian with Urgonian facies, Berger et al. 1978). In this calcareous context, the Cèze River
160 generates a 100m deep canyon of 20km long (Jolivet & Martin, 2008; Chapuis, 2017; Fig. 1). In the
161 canyon, the river is reduced to 20 to 30 m width with a shallow bottom sediment layer (mostly pebbles
162 and gravel of metamorphic origin) and with locally apparent calcareous substratum due to gravel
163 extraction during the 60's and 70's. The surrounding plateau is strongly fractured by several faults due
164 to a rollover anticline structure. These faults favoured an important karstification with losing sectors
165 (noted L1 and L2 on Fig. 1) and lateral springs (noted S1 to S8 in Fig. 1).
166
167 The climate of the region is characterised by a wet season from October to December (mean rainfall
168 of 88 mm/month) and a dry period from June to September (33 mm/month). The hydrology of the
169 Cèze River is thus characterised by extremely changing discharge with three contrasted periods: a low
170 flow period from July to September where the river discharge reaches 0.147 m^3/sec (at the entry of
171 the canyon), a winter and spring period with intermediate discharge (mean value of 10.5 m^3/sec at the
172 entry of the canyon, varying between years from 3.2 to 16.6 m^3/sec) and a period of violent autumn
173 flash floods (called Cévenol episodes, Saulnier & Le Lay, 2009) reaching 2,200 m^3/sec in 2002 (Chapuis,
174 2017). During the studied period, the river discharge varied at the entry of the canyon from 1180
175 m^3/sec in October 2014 to 0.512 m^3/sec in July 2015. In the canyon, the river is partly fed by
176 groundwater that may represent 49% to 68% of the discharge (during intermediate and low flow
177 periods respectively, Chapuis 2017). The inflow of groundwater fed the river through lateral springs
178 (noted S1 to S8 in the Fig. 1) or diffuse upwellings along the banks and gravel bars. Springs are
179 permanent on the left side (S2, S3, S5, S6, S8 in Fig. 1) and temporary on the right (S4, S7, Fig. 1). The
180 diffuse inflow of groundwater through bottom sediment may represent 50% of the total groundwater
181 inputs (e.g. it was estimated to 202 L/sec on a total increase of 394 L/sec in the canyon; Chapuis, 2017).
182 In return, the Cèze River fed the aquifer through losing sections (L1 and L2 in Fig. 1). These losses may
183 represent 80% of the annual discharge, inducing summer drought near L1 and significant decrease of
184 the discharge near L2 (Chapuis, 2017).
185
186 **3-Material and methods**
187 **3.1-Longitudinal profiles of physicochemical characteristics of surface water.**
188 Longitudinal profiles of temperature and electrical conductivity were measured with a multi-
189 parameter probe (HANNA HI 9829) from a small plastic boat equipped with a GPS to locate each
190 measure along the river. Two longitudinal profiles were performed during the spring season. The first
191 one was realised in two distinct sessions on the 14th of May and on the 7th of July 2013 (with a rather
192 similar discharge of 0.5 m^3/sec at the entry of the canyon). Measurements made in July were corrected

193 and reported to a similar upstream level measured in May. The second longitudinal profile was realised
194 on two successive days in early June 2015 (1.19 m^3/sec at the entry of the canyon) a period where all
195 springs were supplied by groundwater except S7. Each campaign of measurements took two days, this
196 duration introduced temporal changes inside the longitudinal profiles. For temperature, the
197 combination of variations between the two successive days and variations during the day length made
198 any corrections very complex. Thermic profiles were thus presented uncorrected with a combination
199 of spatial and temporal trends. Electrical conductivity corrected to 25°C was roughly stable over the
200 day length and the two successive days, because of stable hydrological conditions during the sampling
201 period. All measurements of the profiles were expressed as a distance from an upstream point (Pont
202 de Rochegude) and noted as kilometric points (kp), the studied sector was thus located between kp
203 4.8 and kp 17.5 (Fig. 1).
204
205 **2.2-Concentration of ^{222}Rn in surface and groundwater**
206 ^{222}Rn is produced by the disintegration of the ^{226}Ra parent isotope present in the substratum. A granitic
207 or a metamorphic substratum is a consistent source of ^{222}Rn (e.g. Cook et al., 2006) as well as in soils
208 resulting of limestone degradation (alterites) or in sediment deposits that originate from the
209 metamorphic bedrock (Lamontagne et al., 2007, Bourke et al., 2014). When groundwater is in contact
210 with these substrates, the ^{222}Rn activity accumulates. Conversely, ^{222}Rn activity rapidly decreases in
211 surface water, because of radon disintegration (the ^{222}Rn has a half-life direction of 3.8 days) and
212 degassing to the atmosphere. For surface waters, a ^{222}Rn increase is thus a good tracer of groundwater
213 input (Cook et al., 2006) and a ^{222}Rn decrease in groundwater is, conversely, a good tracer of surface
214 water input (Bourke et al., 2014).
215 The concentrations of ^{222}Rn in the river water was measured along a longitudinal profile from 2-liter
216 samples collected at subsurface every 500 meters. Measurements were performed on air after
217 reaching equilibrium between radon, air and water using two RAD7 portable alpha spectrometers (Kim
218 et al. 2001).
219 To document the ^{222}Rn concentrations in groundwater, supplementary measurements were
220 performed in 4 springs (S1, S3, S4 and S8) at three occasions (March and May 2015 and May 2016) and
221 in the hyporheic water of the river (at kp 10, Fig. 1) in June 2016.
222
223 **3.3-Hyporheic water and fauna**
224 Hyporheic water and fauna were sampled at 17 stations from kp 4.8 to kp 16.8 (Fig. 1) from the 15th
225 to the 19th of July 2013, a period of very low discharge (less than 0.5m^3/sec at the entry of the canyon).
226 The stations were located on side gravel bars. Thirty-four gravel bars were labelled along the studied
227 section and 17 of them were randomly selected as sampling stations (Fig. 1). The first station was

located just upstream the beginning of the canyon and all the others were located inside the canyon (Fig. 1). At each station, water and fauna were sampled at 3 replicate points, located at the downstream end of a gravel bar (an area predicted to be an upwelling zone) to detect the potential inflow of groundwater. The sampling design resulted in a total of 51 hyporheic samples (17 stations × 3 replicates) and 17 surface water samples. Surface water was directly sampled in the river while the hyporheic water and fauna were sampled at the 51 points at a depth of -40 cm under the sediment surface using the Bou-Rouch technique (Bou and Rouch, 1967; Bou, 1974). A perforated metal pipe of 23 mm internal diameter (9 rows of 5 mm diameter holes in a 13 cm band, 4 cm from the distal end of the pipe) was driven into the sediment at each point.

Water temperature (in °C), electrical conductivity (in µS/cm), and dissolved oxygen (mg/L; Hach HQ-40d Multiparameter) were measured directly in the surface water and in the hyporheic water pumped inside the Bou-Rouch pipe using a peristaltic hand pump (Willy A. Bachofen type). Vertical Hydraulic Gradient (in %) was measured as the difference between surface and hyporheic levels. Additional water samples were taken, filtered on GF/F Whatman filters, stored in 40 mL plastic bottles, and kept in insulated containers for the return to the laboratory to measure Na, K, Ca, Mg, Sulphate and Nitrate concentrations (± 0.1 %) with an ionic chromatography (Dionex 1100, conductivity detector).

Hyporheic invertebrates were collected at the same 51 sampling points using the Bou-Rouch sampler; 10 L of water and sediment were pumped and filtered through a 160 µm mesh net. Samples were preserved in the field in 96% alcohol. Invertebrates were sorted in the laboratory under a stereomicroscope (x20) after sieving. Clitellata and most crustaceans (Ostracoda, Cladocera, Isopoda, and Amphipoda) were identified to species level. Planaria, Acheta, Mollusca and most Insects (Ephemeroptera, Plecoptera, Trichoptera, Heteroptera and Coleoptera) were identified to genus level or group of species, while Diptera remained at the family or sub-familly levels. Finally, Nematoda, Hydracarina, Cyclopids and Harpacticids were not further identified (except for *Parastenocaris* sp.). For Clitellata, Isopoda and the stygobite Amphipoda of the genus *Niphargus*, the morphological identification was completed by DNA barcoding (mitochondrial COI for Clitellata, 16S mitochondrial rDNA for Isopoda and 28S nuclear rDNA for *Niphargus*; see details in Marmonier et al., 2019) to ensure tricky morphological identifications and to identify damaged/young individuals.

3.4-Statistical analyses

Principal Component Analysis (PCA) was used to assess the spatial variation in physicochemical characteristics of hyporheic water with 10 parameters (i.e. temperature, Vertical Hydraulic Gradient, electrical conductivity, Mg, Ca, K, Na, SO_4, NO_3 and dissolved oxygen). To avoid a mix between spatial

and temporal changes (i.e. along the week for solutes or along the day for temperature), measurements in the hyporheic water were expressed as a difference with surface water. Differences between the 17 stations (n=51, using replicates inside each station) and between section based on hydrology (i.e. losing or gaining sections, n=17, using stations as replicates inside sections) were tested using one-way ANOVA after log(x+1) transformation when necessary.

Total taxonomic richness and total abundances of the hyporheic fauna, stygobite organisms, micro-crustacean and benthic fauna (sum of Ephemeroptera, Plecoptera, Trichoptera and Coleoptera, noted EPTC) were compared between the 17 stations using one-way ANOVAs (n=51) and between river sections based on their hydrology (i.e. losing or gaining sections) using one-way ANOVAs with stations as replicate measurements in each section (n=17). Three types of river sections were tested: (1) sections defined by surface water profile of electrical conductivity obtained in July 2013 and June 2015, (2) sections using ^{222}Rn concentrations in the surface water in June 2015 and (3) sections defined by the hyporheic water chemistry measured in July 2013. Changes in faunal characteristics observed in July 2013 were related to the ^{222}Rn concentrations measured in June 2015, because similar patterns were observed for electrical conductivity at these two dates. The data were log(x+1) transformed when necessary and tests were performed using ExcelStat 2014, the limit of significance was a p-value of 0.05.

4-Results

4.1-Longitudinal profiles of temperature and electrical conductivity in the surface water

Similar spatial patterns were observed in July 2013 and June 2015 (Fig. 2). The temperature was high upstream of the canyon (i.e. 27.3°C in July 2013 and 28°C in June 2015) and strongly modified just downstream of the S1 spring (with a decrease of 1.0°C in July 2013 and 4°C in June 2015). These decreases were linked to the influx of water from the S1 spring that was colder than the river at both dates (14.8°C and 13.8°C in July 2013 and June 2015, respectively). The temperature irregularly decreased all along the first part of the studied sector until Kp 10 (to 25.8°C in July 2013 and to 21.8°C in June 2015). In the second part of the canyon, different trends were observed between dates. In July 2013, the temperature still decreased to 25.02°C at Kp 16.2. In June 2015, a 2.5°C decrease was observed at Kp 10.2 due to a stop followed by a progressive increase until 24.8°C at Kp 16.8. At both dates, the temperature profiles were strongly disturbed downstream of the S8 spring, with a decrease of 1.1°C and 5.3°C in July 2013 and June 2015 respectively. The temperatures measured in the S8 spring (14.4°C and 14.9°C in July 2013 and June 2015, respectively) were effectively lower than the

298 temperature of the river. The resulting longitudinal patterns in water temperature were not associated
299 to changes in valley width (Fig. 1) but with diffuse inflows of cold water in the first 4 km of the canyon
300 and some very rapid changes at 100m-scale, just downstream of the S1 and S8 springs in July 2013 and
301 June 2015. These rapid changes correspond to groundwater plume downstream of springs (see aerial
302 infrared photographs in Fig. S2). A similar effect was observed for the S5 spring (June 2005) and at a
303 lesser extent near the S7 spring, but no effect was observed for the four other springs
304
305 The pattern in electrical conductivity follows a more repeatable trend in July 2013 and June 2015 (Fig.
306 2). It was low upstream of the canyon (380 µS/cm and 375 µS/cm in July 2013 and June 2015,
307 respectively), but strongly changed just downstream of the S1 spring (increase to 420 or 450 µS/cm)
308 because of the input of highly conductive groundwater (547 and 615 µS/cm in July 2013 and June 2015,
309 respectively). All along the first part of the canyon, from Kp5 to Kp 9, the electrical conductivity
310 regularly increased to a relatively stable value (around 420 µS/cm at both dates) from Kp 10 to Kp 17
311 (noted in blue in the Fig. 2). Few rare and rapid changes were observed (generally less than 20% of the
312 values) just downstream of the S5 and S7 springs. Finally, the electrical conductivity was strongly
313 modified just downstream of the S8 spring, with an increase to 447 µS/cm in July 2013 and to 458
314 µS/cm in June 2015, when the water of the S8 spring reached 442 µS/cm and 510 µS/cm in July 2013
315 and June 2015, respectively (noted in blue in Fig. 2).
316
317 The longitudinal patterns in electrical conductivity were not associated to changes in valley width: no
318 significant inflow of groundwater, with associated low temperature or high electrical conductivity,
319 were measured upstream of the canyon entry (pk 4.8, noted in white in Fig. 2). Conversely, the first
320 part of the canyon (pk 5 to 10) or the downstream end of the studied sector (pk 17) did not show any
321 consistent change in river width, but a decrease in the temperature and an increase in electric
322 conductivity (gaining sections noted in blue in Fig. 2).
323
324 **4.2-Longitudinal pattern of ^{222}Rn concentrations**
325 The concentrations of ^{222}Rn were low at the entrance of the canyon (less than 500 Bq/m^3) and slowly
326 increased all along the first part of the section until Kp 9 where ^{222}Rn reached a maximal value (close
327 to 1000 Bq/m^3, Fig. 3). Downstream, the ^{222}Rn concentrations decreased irregularly until Kp 15 to
328 similar values to those measured upstream of the canyon (close to 400 Bq/m^3, Fig. 3). Finally, the
329 concentrations increased again downstream of the Kp 15 to the end of the studied sector.
330
331 The ^{222}Rn concentrations were high in the karstic groundwater of the region, varying between 1120
332 and 2560 Bq/m^3 in the spring water (S1, S3, S4 and S8). In the same way, the ^{222}Rn concentrations

measured inside the sediment at Kp 10 reached very high values (i.e. ca 14 kBq/m^3 in June 2016). The changes in ^{222}Rn concentrations may be used to locate gaining and losing sections along the studied sector (noted in blue and in white in Fig. 3).

4.3-Hyporheic water chemistry

The PCA performed on the 17 stations (Fig. 4) highlights differences in hyporheic water chemistry that mirror differences in geologic characteristics of the watershed: when entering the canyon, the surface water of the Cèze River is characterised by high concentrations in Mg, K, and Na (Table 1) a consequence of the metamorphic rocks dominating the upper part of the watershed. These parameters have positive coordinates on the PC1 axis (Fig. 4a). In contrast, the groundwater sampled in the karstic springs were characterised by high electrical conductivity and high concentrations in Ca (Table 1) linked to the calcareous substratum. These two parameters have clearly negative coordinates on the PC1 Axis (Fig. 4a). The PC2 axis highlights a reverse pattern between Dissolved Oxygen, Nitrate and Sulphate, with a poor link with the origin of water.

The differences in chemical characteristics of the hyporheic water sampled in the 17 stations result in a gradient of stations along the PC1 axis (Fig. 4b). All sampling stations have positive Vertical Hydraulic Gradients, ranging from a minimum value of +0.4% at stations 24, 27 and 32, to +6.6% at the station 3 and +7.5% at station 34 (Fig. 4e), but there were two types of waters that upwell in the different stations:

- the hyporheic water sampled upstream of the canyon (at station 1, Kp 5), in station 12 and 14 (Kp7.7 and 8.8) and in the second part of the canyon (stations 19 to 33, from Kp 11 to 16.5) was similar to surface water for temperature, K, Mg, Na, and sulphate concentrations (Fig. 4d, f, h), all characteristics of surface water that follow short flow path inside the hyporheic zone before to return to the river (noted in white in Fig. 4b).
- In contrast, the water sampled in the first part of the canyon (stations 3 to 11, 13 and 16, from pk 5 to 10) and at the end of the studied sector (station 34) was cold and with a high electrical conductivity (Fig. 4c, f) thus similar to karstic groundwater or, at least, with a hyporheic water that follows a long flow path inside sediment (noted in blue in Fig. 4b).

4.4-Hyporheic biodiversity

A total of 65,860 individuals and 116 taxa were sampled in the 51 hyporheic samples. For the surface water organisms (63,830 individual and 99 taxa), the dominant organisms were the Naididae (*N. communis* and *N. barbata*), *Alona guttata* and *Vestalenula* sp. for micro-crustaceans, the insect Leuctridae (*L. major* and *L. nigra*), three species of Ephemeroptera (*Procloeon bifidum*, *Caenis* sp. and *Choroterpes picteti*), three species of Coleoptera (*Esolus* sp., *Hydroscapha* sp. and *Yola* sp.) and three

groups of Diptera (Ceratopogonidae, Chironomidae Orthocladiinae and Tanytarsini). The stygobite fauna was less abundant (only 2030 individuals for the 51 samples), but well diversified with 17 species. The most abundant stygobites were the Phallodrilinae *Gianius aquaedulcis* and the Lumbriculidae (cf *Trichodrilus*), the microcrustaceans *Parastenocaris* sp., *Phreatalona phreatica*, *Marmocandona zschokkei* and *Cryptocandona kieferi*, the Amphipoda *Niphargus casparyi* and *N. kochianus* and the Isopoda *Proasellus walteri*.

The total abundance and taxonomic richness of the hyporheic fauna varied significantly with the stations ($F_{(17,36)}$=10.83, p-value=1.7 10^{-9} and $F_{(17,36)}$=4.36, p-value=0.0001 respectively; Fig. 5) with maximum abundances in stations 20 and 24 (with a mean of 2143 and 5760 ind./10L respectively). When stations were grouped into hydrologic sections (i.e. gaining versus losing) the abundances did not significantly vary, whatever the indicator chosen (i.e. longitudinal profile of electrical conductivity, ^{222}Rn concentrations or hyporheic water chemistry; in all cases p-values > 0.05), because of high variability inside each group of stations. On the contrary, the taxonomic richness was significantly higher in gaining sections (23.8 ± 3.8 taxa) than in losing sections (17.2 ± 6.7 taxa) based on ^{222}Rn changes ($F_{(1,16)}$=6.01, p-value=0.027).

Microcrustaceans represented a large proportion of the total abundances of the hyporheic fauna (76 ± 16% of the specimens). Their abundances and taxonomic richness varied significantly with stations ($F_{(17,36)}$=11.87, p-value=5.10^{-10} and $F_{(17,36)}$=3.66, p-value=0.0005, respectively; Fig. 5), with highest values measured at the same stations 20 and 24, just upstream or inside the second losing section (L2 in Fig. 1). Some species were more abundant in losing sections (such as the *Vestalenula* sp. restricted to the stations 1, 24, 25, and 27; Supplementary material Fig. S3), but when all microcrustaceans are considered together, neither the species richness nor the abundances significantly changed between sections defined by their hydrology (i.e. losing vs gaining) whatever the indicator chosen (i.e. longitudinal profiles of electrical conductivity, ^{222}Rn concentrations, hyporheic water chemistry; in all cases p-value > 0.05).

The abundances and richness of benthic EPTC (Fig. 5) did not vary significantly with stations (p-value > 0.05), but with sections based on ^{222}Rn concentrations. The EPTC were two times more abundant in the gaining sectors (mean of 48.5 individuals/10L) than in losing (17.7 individuals/10L; $F_{(1,16)}$ = 4.92, p-value = 0.042) and showed higher taxonomic richness in gaining (mean of 3.9 taxa) than in losing sections (2.4 taxa; $F_{(1,16)}$ = 5.09, p-value = 0.039). These patterns were explained by a clear preference for gaining stations of the Plecoptera *Leuctra* spp. (L. *major* and L. *nigra*), the Ephemeroptera *Choroterpes picteti* and the Coleoptera *Esolus* sp. (Supplementary material Fig. S3). The differences in

EPTC abundances and taxonomic richness disappeared when the delineation of hydrological sections was based on the electrical conductivity profile or the hyporheic water chemistry.

Similarly, the abundances and species richness of the stygobite fauna (Fig. 5) did not vary between stations, but abundances significantly changed when stations were grouped according to their hydrology (i.e. gaining vs losing). Stygobites were more abundant in gaining sections (i.e. 55.4 ± 48.7 individuals/10L) than in losing sections (16.9 ± 11.9 individuals/10L) when sections were based on ^{222}Rn changes ($F_{(1,15)}$ = 7.002, p-values = 0.0018) or electric conductivity profiles ($F_{(1,15)}$ = 6.797, p-values = 0.019). Some stygobite species showed a clear preference for gaining sections. For example, the ostracods *Marmocandona zschokkei* and *Cryptocandona kieferi*, the Amphipods *Niphargus kochianus* and *N. fontanus* were all restricted or more abundant in the gaining sections of the river (Supplementary material Fig. S3) and the karstic Amphipod *N. virei* only occurred at the station 33. When the group of stations were built using hyporheic water characteristics, neither the stygobite abundances nor the stygobite taxonomic richness varied significantly between gaining and losing sections (p-value>0.05).

5-Discussion

The location of gaining and losing sections along a 13-km section of a Mediterranean karstic river, such as the Cèze River, is difficult because of the complexity of interactions between the geological heterogeneities of the substratum, the complex tectonics, the local geomorphologic features and the hydrology that constitute altogether a single karst-river system comparable to the stygoscape described for alluvial rivers by Ward (1997) or Datry et al. (2008). When a general model of the spatial distribution of river - groundwater exchanges (based on an alluvial river and a porous aquifer; Toth, 1963; Dole-Olivier et al., 1993; Capderrey et al., 2013) is applied to this karstic river, only a part of the hypotheses proposed at the beginning of the study was supported by the results. In this study, we observed that the inflow of karstic groundwater modified the surface water chemistry (H1 validated), the gravel bar tails were upwelling zones with positive Vertical Hydraulic Gradient (first part of H2 validated), and the link between groundwater inflows and stygobite abundances in the hyporheic zone was effectively observed in the karstic canyon of the Cèze River (H3 validated). Another original result of this study is the link between the ^{222}Rn concentration profiles in surface water and the occurrence of groundwater fauna in the river sediment. Two hypotheses were rejected (i.e. the gaining sections located upstream of valley narrowing –second part of H2 - and the occurrence of benthic EPTC fauna in the losing stations –H4). These rejections highlight some specificities of karstic rivers and Mediterranean rivers in their relation with surrounding groundwater that must be accounted for in river management.

438 **5.1- Groundwater inflow and surface water chemistry**

439 As predicted by the first hypothesis, the inflows of groundwater from the karstic systems were strong
440 enough to modify the chemical characteristics of the Cèze surface water. This influence was not always
441 clear for the longitudinal changes in temperature. Thermal profiles may be modified by several
442 environmental changes without relation to groundwater dynamics (e.g. shaded area, temporal
443 changes along the day cycle..., Wawrzyniak et al., 2017). In contrast, the electrical conductivity
444 appeared to be a very consistent indicator of groundwater inflow in the Cèze River, with regular
445 increase along the first part of the canyon and close to the spring S8 and a relative stability elsewhere.
446 These types of longitudinal profiles of electrical conductivity were frequently observed in rivers, for
447 example in the Murray River (Simpson & Herczeg, 1991) or the Cockburn River (Cook et al., 2006). In
448 the case of the Cèze River, the electrical conductivity was particularly relevant because of the
449 contrasted origin of the surface water (linked to the upstream metamorphic watershed) and of the
450 groundwater (linked to the karstic area).
451
452 Another surface water characteristic that changed along the studied sector was the concentration of
453 ^{222}Rn. This radioactive isotope was already used to locate groundwater upwelling in rivers (Ellins et al.,
454 1990; Wu et al., 2004; Cook et al., 2006). The Cèze River offered a particularly interesting geological
455 context for the use of ^{222}Rn: the bed sediments are of metamorphic origin (mostly dominated by
456 gneisses and quartzites, Chapuis, 2017) surrounded by a karstic system with alterite deposits. The
457 water flowing in karstic systems was enriched in ^{222}Rn that ranged from 1120 to 2560 Beq/m^3
458 (according to measurements in springs). In the same way, the hyporheic water was also strongly
459 enriched in ^{222}Rn (until 14 kBq/m^3 at station 16) certainly because of the metamorphic origin of the
460 river sediment. The mix of karstic groundwater and deep hyporheic water that upwells in the river may
461 explain the changes in ^{222}Rn concentration in gaining sections. In contrast, the ^{222}Rn in the losing
462 sections decreased through disintegration and release to the atmosphere and the concentration in
463 surface water returns to upstream concentrations (Cook, 2013). The ^{222}Rn concentration turned out as
464 a possible indicator of deep groundwater reaching the river, at least in this geological context with
465 metamorphic sediment layer in a calcareous context.
466
467 **5.2-Location of river-groundwater exchange zones**

468 The location of large-scale gaining and losing sections is an increasing concern for alluvial rivers, where
469 several methods were proposed based on hydraulic head measurements in several mini-piezometers
470 (i.e. measurement of relative groundwater level, Kasahara & Wondzell, 2003), longitudinal profiles of
471 water chemistry (Cook, 2013; Guida et al., 2013) or thermal infra-red images (Wawrzyniak et al., 2013,
472 2016). In karstic rivers, few studies focus on the location of diffuse karstic inflows to river compared to

473 large karstic springs (e.g. Rugel et al., 2016). The present study confirms the changes in the discharge
474 observed by Chapuis (2017): the karstic inflows were not limited to large springs, but also occurred
475 through diffusive inflows along large sections of the river, at least along a 4km-long section in the
476 upstream part of the canyon.
477
478 At the scale of the geomorphological units, all downstream ends of the studied gravel bars were
479 upwelling zones (in all cases Vertical Hydraulic Gradient had positive values, the first part of H2
480 validated), even if upwelling zones were fed by different types of water in gaining or losing sections.
481 At the scale of the geological context, the predicted influence of valley width reduction on
482 groundwater inflow (the second part of H2) was not verified. The most significant reduction in valley
483 width is located just upstream of the canyon entrance, where a hydrological study highlighted a losing
484 section (noted L1 in Fig. 1; Chapuis, 2017). In these sections (where station 1 is located), the hyporheic
485 water that upwells into the river was extremely similar to river water suggesting short flowpaths inside
486 the sediment.
487
488 The sections with the most intense groundwater inflow were not linked to changes in canyon width,
489 but were associated to karstic spring (see electrical conductivity changes close to S1 and S8, Fig. 2), but
490 also to hidden diffuse groundwater inputs (see electrical conductivity and ^{222}Rn concentration changes
491 in the upstream part of the canyon, Fig. 3). Chapuis (2017) evaluated groundwater contribution to the
492 Cèze River discharge to 49 to 68% (for intermediate and low discharge, respectively), but only the half
493 of this contribution was explained by the spring discharge, the other half may have originated from
494 diffuse inflow through the bed sediment (Chapuis, 2017). This result is important for river management
495 because large springs are generally the only groundwater inflows taken into account in management
496 plans (e.g. protection of groundwater against excessive pumping or pollution), while the gaining
497 sections of diffuse groundwater are frequently ignored and may represent a crucial objective for
498 resource protection.
499
500 **5.3-The response of the hyporheic fauna**
501 The total taxonomic richness of hyporheic assemblages varied between sections, with higher richness
502 in the gaining area, while no differences were observed for total abundances because of very high
503 differences between stations, resulting in highly variable microcrustacean abundances. Some stations
504 (i.e. 20 and 24) were highly populated by a large set of species, especially by microcrustaceans. In these
505 two stations, the abundances of the ostracod *Vestalenula* sp. were the highest. This Darwinulidae
506 genus pertains to a group of subtropical Ostracoda (Artheau, 2007) and is certainly thermophilous.
507 These stations 20 and 24 were located close to a losing section of the river and showed very high

temperatures in their hyporheic water (e.g. 27°C in station 24) that may explain this strong development of hyporheic microcrustaceans (Dole-Olivier et al., 2000).

In contrast with microcrustaceans, the abundances of benthic EPTC was not higher in losing stations (H4 rejected). In the Cèze River, the EPTC species colonised preferably the hyporheic zone fed by groundwater in gaining sections defined by changes in ^{222}Rn concentrations, both for abundances and species richness. This result was not predicted because the benthic fauna generally develops abundant populations in well-oxygenated hyporheic zone rich in labile organic matter (Dole-Olivier & Marmonier, 1992; Capderrey et al., 2013), all characteristics found in losing sections (Claret et al., 1998). In a Mediterranean river, such as the Cèze river, the losing sections with high temperatures may be a disadvantage to large benthic fauna like EPTC. In contrast, the low water temperature and the oligotrophy of the groundwater that upwells inside the river in gaining sections may represent a favourable habitat for benthic invertebrates with cold water preferences (e.g. *Esolus* sp. or *Leuctra major*, Bertrand, 1965; Berthelemy, 1968).

In the same way, the abundances of the stygobites were significantly higher in the stations grouped in gaining sections, as predicted in the third hypothesis. The links between hyporheic water characteristics and stygobites are now rather well documented (Dole-Olivier & Marmonier, 1992; Datry et al., 2008): the stygofauna generally colonised areas with a constant temperature and oligotrophic water, with low exigency for dissolved oxygen and fresh organic matter (Malard & Hervant, 1999), they thus develop dense populations in upwelling zones (Dole-Olivier & Marmonier, 1992). Here, the stygobite fauna was more abundant or even restricted to the gaining sections (i.e. the first part of the canyon and around the S8 spring) where the hyporheic water had low temperatures (e.g. 15.5 and 17.7°C at stations 3 and 34, respectively) and high dissolved oxygen contents (e.g. 8.6 and 6.1 mg/L at stations 3 and 34, respectively).

This study highlighted the crucial role of gaining sections in the biological functioning of a Mediterranean river: the river sediment fed by groundwater upwelling represents an attractive habitat for a part of the invertebrates. The total taxonomic richness, the abundances of stygobite fauna and the benthic EPTC were higher in the gaining than in the losing sections. They can be considered as hotspots for invertebrate biodiversity in rivers and must be protected (Boulton, 2000).

5.4-Using surface water characteristics to predict hyporheic biodiversity.

Hotspots in hyporheic biodiversity may be endangered by several human activities that modify sediment characteristics and exchanges with groundwater (e.g. groundwater pumping, dam building,

543 change in the river hydrology...; Boulton, 2000). Although they need protection (Gibert & Culver, 2009),
544 the location of these hotspots remains difficult. This study demonstrates that longitudinal profiles in
545 surface water chemistry using simple (e.g. electrical conductivity) or more complex describers (e.g.
546 ^{222}Rn) may be used to predict the changes in hyporheic biodiversity. The prediction was based on a
547 segmentation of the river in sections with contrasted hydrology (i.e. gaining and losing sections), but
548 this segmentation may vary according to the indicator used (Table 2).
549
550 The longitudinal profiles of surface water temperature measured from a canoe using a thermic probe
551 gave poor results. The two profiles presented in this study were difficult to analyse and do not fit with
552 faunal distribution certainly because of the duration of the measurement (at least two successive days)
553 that mixed the temporal changes with the thermic trends linked to groundwater upwelling zones. To
554 avoid this problem, infra-red images took by a ULM or a drone may reduce the duration of the
555 measurement and make more consistent the longitudinal profile (Hare et al., 2015; Wawrzyniak et al.,
556 2013, 2016; Dole-Olivier et al., 2019).
557
558 In the same way, the segmentation of the studied sector using hyporheic water characteristics gave
559 highly fragmented sections (see Fig. 4 and Table 2) that poorly fit with the longitudinal distribution of
560 hyporheic fauna (i.e. the total hyporheic fauna, the EPTC or the stygobionts did not significantly
561 changed with sections defined by hyporheic water chemistry). This discrepancy may be surprising, but
562 already reported for another Mediterranean river, the Drôme River (Marmonier et al., 2019). In these
563 two rivers, the hyporheic assemblages appeared a more integrative and reliable indicator of
564 groundwater upwelling than hyporheic water chemistry that may locally change for light
565 geomorphologic or geologic differences.
566
567 The longitudinal profiles of electrical conductivities in the surface water were similar in July 2013 and
568 June 2015. These profiles were consistent with the profile of ^{222}Rn concentrations obtained in June
569 2015: two losing sections were located upstream of the canyon entrance and in its central part, two
570 gaining sections were observed in the first part of the canyon and close to the last S8 spring. The
571 stygobite fauna and the EPTC followed very similar patterns, with significant differences in their
572 abundances in sections where electrical conductivity and ^{222}Rn concentrations increased in surface
573 water (i.e. gaining sections). This is the first time that these three types of indicators were used in the
574 same sector of a river, even if the hyporheic fauna and the ^{222}Rn concentrations were measured at two
575 different dates (i.e. July 2013 and June 2015, respectively). The ^{222}Rn concentrations were measured
576 at the same time as the second electrical conductivity profile, that gave similar spatial trends with the
577 first one, but this temporal interval remains a limit of this study. The link between hyporheic fauna and

surface water characteristics look promising for location of potential hotspots of hyporheic biodiversity (Table 2). Future research must focus on the possible use of ^{222}Rn indicator in other geological contexts, keeping in mind that each type of indicator brought a complementary image of the functioning of the karst-river system. Altogether, the five indicators used concomitantly in this study showed high efficiency for the location of gaining sections that could help managers to define optimal protection strategies for hyporheic biodiversity and, more globally, for the river integrity.

Acknowledgements: This work was funded by the Rhone River Water Agency (Agence de l'Eau Rhône Méditerranée et Corse, conventions 2013-2900 and 2015-1668) in the framework of the ZABR (LTSER Rhone River Basin). We thank the Ecole Universitaire de Recherche H2O'Lyon, Thérèse Bastide (ENTPE) for water chemical analyses and Mathilde Novel for help during field work. We also thank Hughes Brenteganni (Syndicat Mixte de la Rivière Cèze, ABCèze) and Joël Jolivet (UMR "Espace" University of Nice-Sophia-Antipolis) for exchanges on the geology and hydrology of the studied sector. English editing was performed by Landmark Academic Proofreading (London, UK).

References

Artheau, M., 2007. Geographical review of the ostracod genus *Vestalenula* (Darwinulidae) and a new subterranean species from southern France. Invertebrate Systematics, 21, 471-486.

Baxter, C., Hauer, F. R., & Woessner, W. W., 2003. Measuring groundwater–stream water exchange: new techniques for installing minipiezometers and estimating hydraulic conductivity. Transactions of the American Fisheries Society, 132, 493-502.

Berger, G., Lefebvre, A., Turc, R., Gras, H., Poidevin, J.-L., Arène, J., Guérangé, B., Pellet, J., 1978. Carte géologique de la France au 1/50 000e – Feuille d'Alès n° 912. Bureau de Recherches Géologiques et Minières (Ed).

Berthélemy, C., 1968. Contribution à la connaissance des leuctridae [Plecoptera]. In Annales de Limnologie-International Journal of Limnology, 4, 175-198.

Bertrand, H., 1965. Récoltes de coléoptères aquatiques dans les régions montagneuses de l'Espagne: observations écologiques (Dryopidae, Elminthinae, Helmiinae Auct.). Annales de Limnologie-International Journal of Limnology, 1, 245-255.

Bou, C., 1974. Les méthodes de récolte dans les eaux souterraines interstitielles. Annales de Spéléologie 29, 611-619.

Bou, C., Rouch, R., 1967. Un nouveau champ de recherches sur la faune aquatique souterraine. Compte-Rendu Académie des Sciences, 265, 369-370.

Boulton, A. J., 2000. River ecosystem health down under: assessing ecological condition in riverine groundwater zones in Australia. Ecosystem Health, 6, 108-118.

Bourke, S. A., Cook, P. G., Shanafield, M., Dogramaci, S., Clark, J. F., 2014. Characterisation of hyporheic exchange in a losing stream using radon-222. Journal of Hydrology, 519, 94-105.

Brunke, M., Gonser, T.O.M., 1999. Hyporheic invertebrates: the clinal nature of interstitial communities structured by hydrological exchange and environmental gradients. Journal of the North American Benthological Society 18, 344-362.

Capderrey, C., Datry, T., Foulquier, A., Claret, C., Malard, F., 2013. Invertebrate distribution across nested geomorphic features in braided-river landscapes. Freshwater Science 32, 1188-1204.

Chapuis H., 2017. Caractérisation, Evaluation, Modélisation des échanges entre aquifères karstiques et rivières : application à la Cèze (Gard, France). Thesis University of Lyon, 466p.

Claret, C., Fontvieille, D., 1997. Characteristics of biofilm assemblages in two contrasted hydrodynamic and trophic contexts. Microbial Ecology, 34, 49-57.

Claret, C., Marmonier, P., Bravard, J. P., 1998. Seasonal dynamics of nutrient and biofilm in interstitial habitats of two contrasting riffles in a regulated large river. Aquatic Sciences, 60, 33-55.

627 Cook, P. G., Lamontagne, S., Berhane, D., Clark, J. F., 2006. Quantifying groundwater discharge to
628 Cockburn River, southeastern Australia, using dissolved gas tracers 222Rn and SF6. Water
629 Resources Research, 42, 1-12.
630 Cook, P. G., 2013. Estimating groundwater discharge to rivers from river chemistry surveys.
631 Hydrological Processes, 27, 3694-3707.
632 Creuzé des Châtelliers, M. C. D., Reygrobellet, J. L., 1990. Interactions between geomorphological
633 processes, benthic and hyporheic communities: First results on a by-passed canal of the french
634 upper Rhône River. Regulated Rivers: Research & Management, *5*, 139-158.
635 Datry, T., Scarsbrook, M., Larned, S., Fenwick, G., 2008. Lateral and longitudinal patterns within the
636 stygoscape of an alluvial river corridor. Fundamental and Applied Limnology-Archiv für
637 Hydrobiologie, 171, 335-347.
638 Davy-Bowker, J., Sweeting, W., Wright, N., Clarke, R. T., Arnott, S., 2006. The distribution of benthic
639 and hyporheic macroinvertebrates from the heads and tails of riffles. Hydrobiologia, *563*, 109-
640 123.
641 Deutsch, B., Mewes, M., Liskow, I., Voss, M., 2006. Quantification of diffuse nitrate inputs into a small
642 river system using stable isotopes of oxygen and nitrogen in nitrate. Organic geochemistry, 37,
643 1333-1342.
644 Doering, M., Uehlinger, U., Rotach, A., Schaepfer, D.R., Tockner, K., 2007. Ecosystem expansion and
645 contraction dynamics along a large alpine alluvial corridor (Tagliamento River, Northeast Italy).
646 Earth Surface Processes and Landforms: The Journal of the British Geomorphological Research
647 Group 32, 1693-1704.
648 Dole-Olivier, M. J., 1998. Surface water–groundwater exchanges in three dimensions on a backwater
649 of the Rhône River. Freshwater biology, 40, 93-109.
650 Dole-Olivier, M. J., Marmonier, P., 1992. Patch distribution of interstitial communities: prevailing
651 factors. Freshwater Biology, 27, 177-191.
652 Dole-Olivier, M. J., Creuzé des Châtelliers, C., Marmonier, P., 1993. Repeated gradients in subterranean
653 landscape--example of the stygofauna in the alluvial floodplain of the Rhone River(France).
654 Fundamental and Applied Limnology-Archiv für Hydrobiologie, 127, 451-471.
655 Dole-Olivier, M. J., Galassi, D. M. P., Marmonier, P., Creuzé des Châtelliers, M., 2000. The biology and
656 ecology of lotic microcrustaceans. Freshwater biology, 44, 63-91.
657 Ellins, K. K., Roman-Mas, A., Lee, R., 1990. Using 222Rn to examine groundwater/surface discharge
658 interaction in the Rio Grande de Manati, Puerto Rico. Journal of Hydrology, 115, 319-341.
659 Ford, T. E., Naiman, R. J., 1989. Groundwater–surface water relationships in boreal forest watersheds:
660 dissolved organic carbon and inorganic nutrient dynamics. Canadian Journal of Fisheries and
661 Aquatic Sciences, 46, 41-49.

662 Gibert, J., Culver, D. C., 2009. Assessing and conserving groundwater biodiversity: an introduction.
663 Freshwater Biology, 54, 639-648.
664 Graillot, D., Paran, F., Bornette, G., Marmonier, P., Piscart, C., Cadilhac, L., 2014. Coupling groundwater
665 modelling and biological indicators for identifying river/aquifer exchanges. SpringerPlus, 3, 68.
666 Grasby, S. E., Hutcheon, I., McFarland, L., 1999. Surface-water–groundwater interaction and the
667 influence of ion exchange reactions on river chemistry. Geology, 27, 223-226.
668 Guida, M., Guida, D., Guadagnuolo, D., Cuomo, A., Siervo, V., 2013. Using Radon-222 as a Naturally
669 Occurring Tracer to investigate the streamflow-groundwater interactions in a typical
670 Mediterranean fluvial-karst landscape: the interdisciplinary case study of the Bussento river
671 (Campania region, Southern Italy). WSEAS Transaction on Systems, 12, 85-104.
672 Hare, D. K., Briggs, M. A., Rosenberry, D. O., Boutt, D. F., Lane, J. W., 2015. A comparison of thermal
673 infrared to fiber-optic distributed temperature sensing for evaluation of groundwater discharge
674 to surface water. Journal of Hydrology, 530, 153-166.
675 Hayashi, M., Vogt, T., Mächler, L., Schirmer, M., 2012. Diurnal fluctuations of electrical conductivity in
676 a pre-alpine river: Effects of photosynthesis and groundwater exchange. Journal of Hydrology,
677 450, 93-104.
678 Hendricks, S. P., White, D. S., 1988. Hummocking by lotic *Chara*: observations on alterations of
679 hyporheic temperature patterns. Aquatic Botany, 31, 13-22.
680 Jolivet, J., Martin, C., 2008. La morphologie karstique dans le canyon de la Cèze et sur le plateau de
681 Méjannes-le-Clap (Garrigues nord, Gard, France). Rapports avec l'évolution paléogéographique
682 mio-pliocène. Physio-Géo. Géographie Physique et Environnement, 2, 53-75.
683 Kasahara, T., Wondzell, S. M., 2003. Geomorphic controls on hyporheic exchange flow in mountain
684 streams. Water Resources Research, 39, SBH-3.
685 Kim, G. C., Burnett, W. C., Dulaiova, H., Swarzenski, P. W., Moore, W. S. , 2001. Measurement of ^{224}Ra
686 and ^{226}Ra Activities in natural waters using a Radon-in-Air Monitor. Environ. Sci. Technol., 35,
687 4680-4683.
688 Lamontagne, S., Cook, P. G., 2007. Estimation of hyporheic water residence time in situ using ^{222}Rn
689 disequilibrium. Limnology and Oceanography: Methods, 5, 407-416.
690 Malard, F., Tockner, K., Dole-Olivier, M. J., Ward, J. V., 2002. A landscape perspective of surface–
691 subsurface hydrological exchanges in river corridors. Freshwater Biology, 47, 621-640.
692 Malard, F., Uehlinger, U., Zah, R., Tockner, K., 2006. Flood-pulse and riverscape dynamics in a braided
693 glacial river. Ecology, 87, 704-716.
694 Marmonier, P., Archambaud, G., Belaidi, N., Bougon, N., Breil, P., Chauvet, E., Claret C., Cornut J., Datry
695 T., Dole-Olivier M.-J., Dumont B., Flipo N., Foulquier A., Gérino M., Guilpart A., Julien F., Maazouzi
696 C., Martin D., Mermillod-Blondin F., Montuelle B., Namour Ph., Navel S., Ombredane D., Pelte T.,

Piscart C., Pusch M., Stroffek S., Robertson A., Sanchez-Pérez J.-M., Sauvage S., Taleb A., Wantzen M., Vervier Ph., 2012. The role of organisms in hyporheic processes: gaps in current knowledge, needs for future research and applications. Annales de Limnologie-International Journal of Limnology 48, 253-266.

Marmonier, P., Olivier, M. J., des Châtelliers, M. C., Paran, F., Graillot, D., Winiarski, T., Konecny-Dupré L., Navel S., Cadilhac, L., 2019. Does spatial heterogeneity of hyporheic fauna vary similarly with natural and artificial changes in braided river width? Science of The Total Environment, 689, 57-69.

Rouch, R., 1992. Caractéristiques et conditions hydrodynamiques des écoulements dans les sédiments d'un ruisseau des Pyrénées. Implications écologiques. Stygologia, 7, 13-25.

Rugel, K., Golladay, S. W., Jackson, C. R., Rasmussen, T. C., 2016. Delineating groundwater/surface water interaction in a karst watershed: Lower Flint River Basin, southwestern Georgia, USA. Journal of Hydrology: Regional Studies, 5, 1-19.

Saulnier, G. M., Le Lay, M., 2009. Sensitivity of flash-flood simulations on the volume, the intensity, and the localization of rainfall in the Cévennes-Vivarais region (France). Water Resources Research, 45, W10425.

Schaller, M. F., Fan, Y., 2009. River basins as groundwater exporters and importers: Implications for water cycle and climate modeling. Journal of Geophysical Research: Atmospheres, 114, 1-21.

Simpson, H. J., Herczeg, A. L., 1991. Salinity and evaporation in the River Murray basin, Australia. Journal of Hydrology, 124, 1-27.

Sophocleous, M., 2002. Interactions between groundwater and surface water: the state of the science. Hydrogeology journal, 10, 52-67.

Stanford, J. A., Ward, J. V., 1993. An ecosystem perspective of alluvial rivers: connectivity and the hyporheic corridor. Journal of the North American Benthological Society, 12, 48-60.

Stanley, E. H., Boulton, A. J., 1993. Hydrology and the distribution of hyporheos: perspectives from a mesic river and a desert stream. Journal of the North American Benthological Society, 12, 79-83.

Tonolla, D., Acuna, V., Uehlinger, U., Frank, T., Tockner, K., 2010. Thermal heterogeneity in river floodplains. Ecosystems, 13, 727-740.

Toth, J., 1963. A theoretical analysis of groundwater flow in small drainage basins. Journal of geophysical Research, 68, 4795-4812.

Ward, J. V., 1997. An expansive perspective of riverine landscapes: pattern and process across scales. GAIA-Ecological Perspectives for Science and Society, 6, 52-60.

Wawrzyniak, V., Piégay, H., Poirel, A., 2012. Longitudinal and temporal thermal patterns of the French Rhône River using Landsat ETM+ thermal infrared images. Aquatic sciences, 74, 405-414.

731 Wawrzyniak, V., Piégay, H., Allemand, P., Vaudor, L., Grandjean, P., 2013. Prediction of water
732 temperature heterogeneity of braided rivers using very high resolution thermal infrared (TIR)
733 images. International Journal of Remote Sensing, 34, 4812-4831.
734 Wawrzyniak, V., Piégay, H., Allemand, P., Vaudor, L., Goma, R., Grandjean, P., 2016. Effects of
735 geomorphology and groundwater level on the spatio-temporal variability of riverine cold water
736 patches assessed using thermal infrared (TIR) remote sensing. Remote Sensing of Environment,
737 175, 337-348.
738 Wawrzyniak, V., Allemand, P., Bailly, S., Lejot, J., Piégay, H., 2017. Coupling LiDAR and thermal imagery
739 to model the effects of riparian vegetation shade and groundwater inputs on summer river
740 temperature. Science of the Total Environment, 592, 616-626.
741 Winter, T. C., 1995. Recent advances in understanding the interaction of groundwater and surface
742 water. Reviews of Geophysics, 33, 985-994.
743 Wu, Y., Wen, X., Zhang, Y., 2004. Analysis of the exchange of groundwater and river water by using
744 Radon-222 in the middle Heihe Basin of northwestern China. Environmental Geology, 45, 647-
745 653.
746
747
748

749 Table 1. Physico-chemical characteristics of the surface water of the Cèze River upstream of the canyon
750 and of four karstic springs in July 2013.
751

	Surface water Mean ± SD n=4	Spring water Mean ± SD n=4	ANOVA test
Temperature (°C)	24.2 ±0.2	15.9 ±1.6	F = 89.6 *p-value* = 0.00008
Electric Conductivity (µS/cm)	332.7 ±6.4	492 ±65.4	F = 23.60 *p-value* = 0.0028
Dissolved Oxygen (mg/L)	8.2 ±0.8	7.7 ±4.2	n.s.
Sulphate (mg/L)	38.9 ±17.2	38.0 ±18.8	n.s.
Nitrate (mg/L)	1.7 ±0.2	29.0 ±42.1	n.s.
Na (mg/L)	15.6 ±1.8	6.0 ±3.7	F = 22.56 *p-value* = 0.0031
K (mg/L)	1.8 ±0.6	1.0 ±0.5	F = 6.17 *p-value* = 0.047
Mg (mg/L)	9.2 ±0.4	3.0 ±2.6	F = 18.71 *p-value* = 0.0049
Ca (mg/L)	41 ±1.3	62.0 ±15.2	F = 7.55 *p-value* = 0.033

752
753
754

Table 2. Suitability of the five describers for the study of groundwater-river exchanges (with usable information for location noted by X).

	GW to river	River to GW	Intensity of exchanges	Estimation of the surfaces	Biodiversity hotspot delineation
Surface water temperature	X		X		
Surface electric conductivity	X		X	X	X
Surface ^{222}Rn concentration	X		X	X	X
Hyporheic water characteristics	X	X	X		
Hyporheic invertebrate composition	X	X			X

Figures

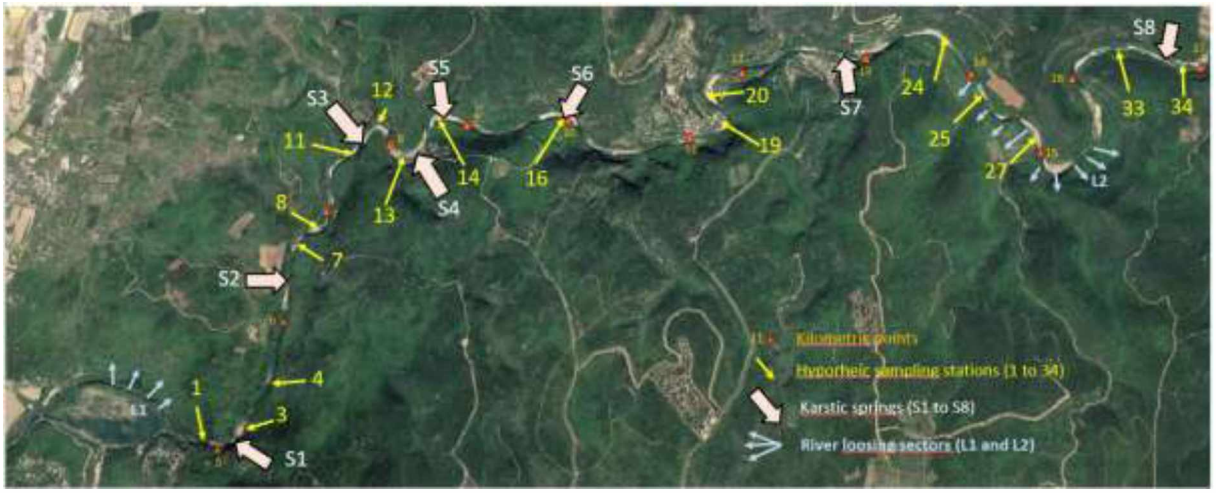

Figure 1. Aerial photograph of the studied sector of the Cèze River (modified from Géoportail, IGN). With distances from upstream to downstream (kilometric points, triangles), location of the 17 hyporheic sampling stations (with gravel bar number, yellow arrows), the 8 karstic springs (beige arrows) and the 2 loosing sectors (blue arrows).

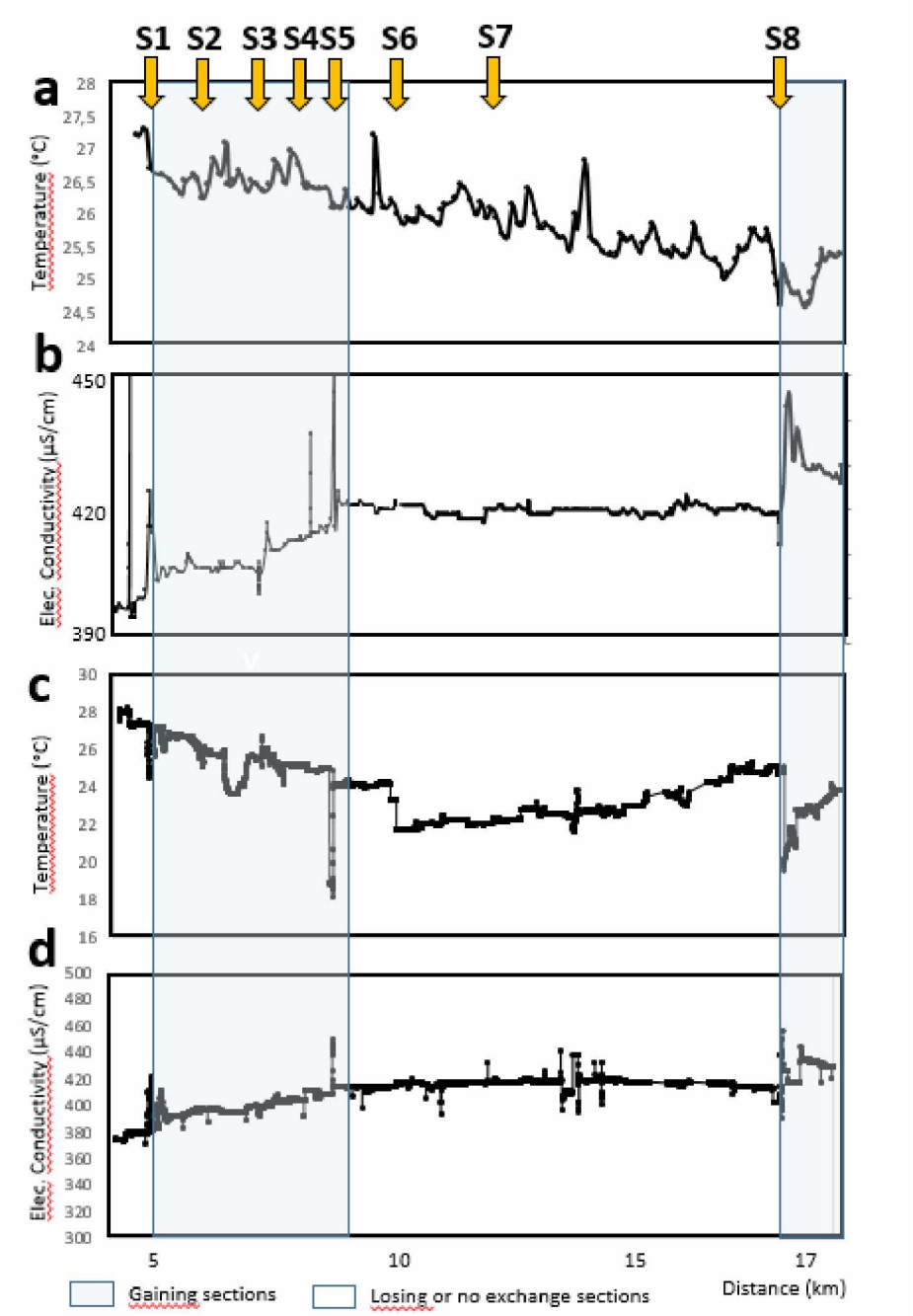

773

774 Figure 2. Longitudinal profiles of temperature (a, for May and July 2013 and c, for June 2015) and of
775 electric conductivity (b, for May and July 2013 and d, for June 2015). Blue and white squares
776 represent the gaining and losing (or no exchange) sections respectively.

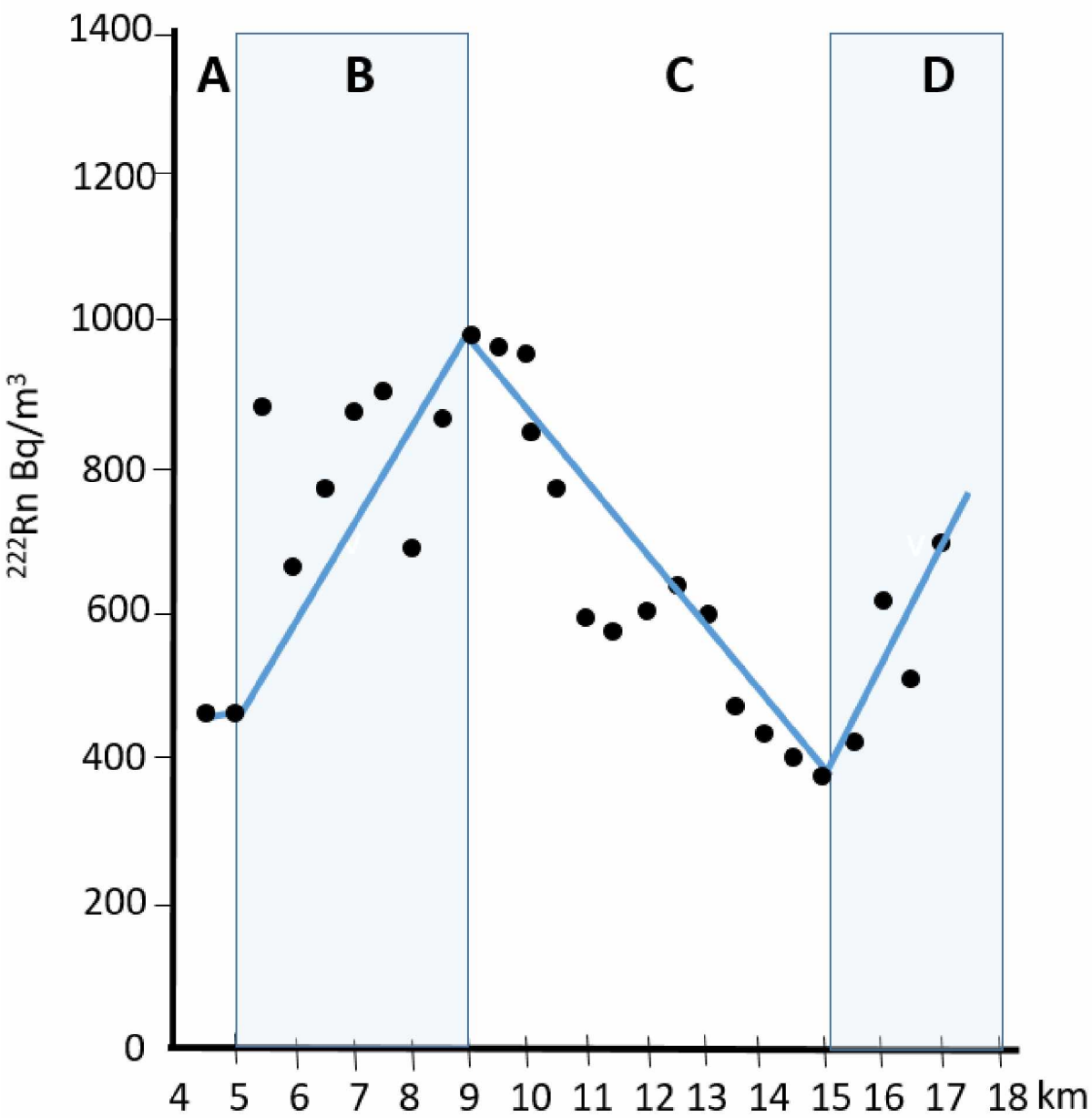

777

778 Figure 3. Longitudinal profile ^{222}Rn in June 2015. Individual measurements (black dots) and lines for
779 the minimum-maximum values. Blue and white squares represent the gaining and losing (or no
780 exchange) sections respectively.

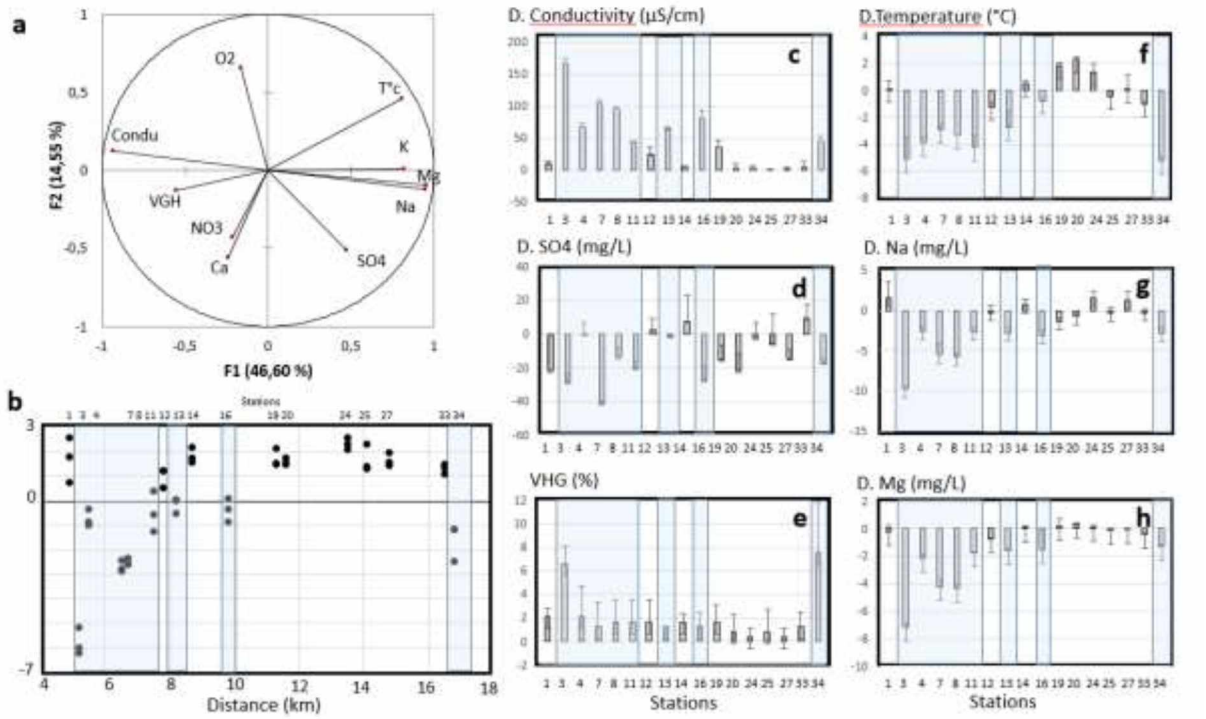

781

782 Figure 4. Chemical characteristics of the hyporheic water in the 17 sampled gravel bars (50cm deep
783 inside sediment). Correlation circle of the PCA (a) and location of the sampling station on the PC1 axis
784 (b; dots are the 3 replicate samples). Chemical variables expressed as the mean difference (D.)
785 between surface water and groundwater for electric conductivity (c), sulphate concentrations (d),
786 Vertical Hydraulic Gradient, VHG (e), temperature (f), Sodium (g) and Magnesium (h; Mean ±
787 Standard Deviation, n=3). Blue squares highlight the stations with negative coordinates on the PC1
788 axis fed by water chemically close to groundwater.

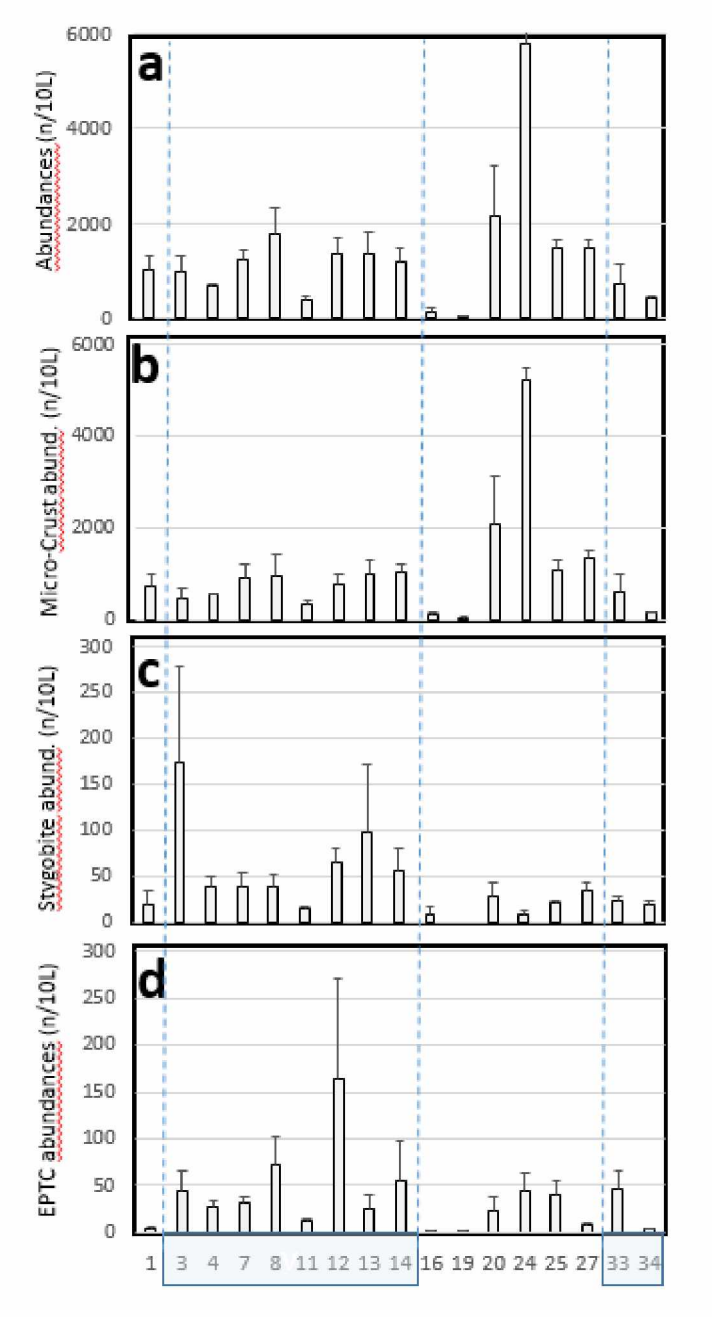

789

790 Figure 5. Hyporheic fauna: total abundances (a), stygobite abundances (b), microcrustacean
791 abundances (c) and benthic species of Ephemeroptera, Plecoptera, Trichoptera and Coleoptera (d) in
792 the 17 stations (from gravel bar 1 to 34). Blue squares represent the gaining sections according to ^{222}Rn
793 concentrations in surface water.

794

795

SUPPLEMENTARY MATERIAL

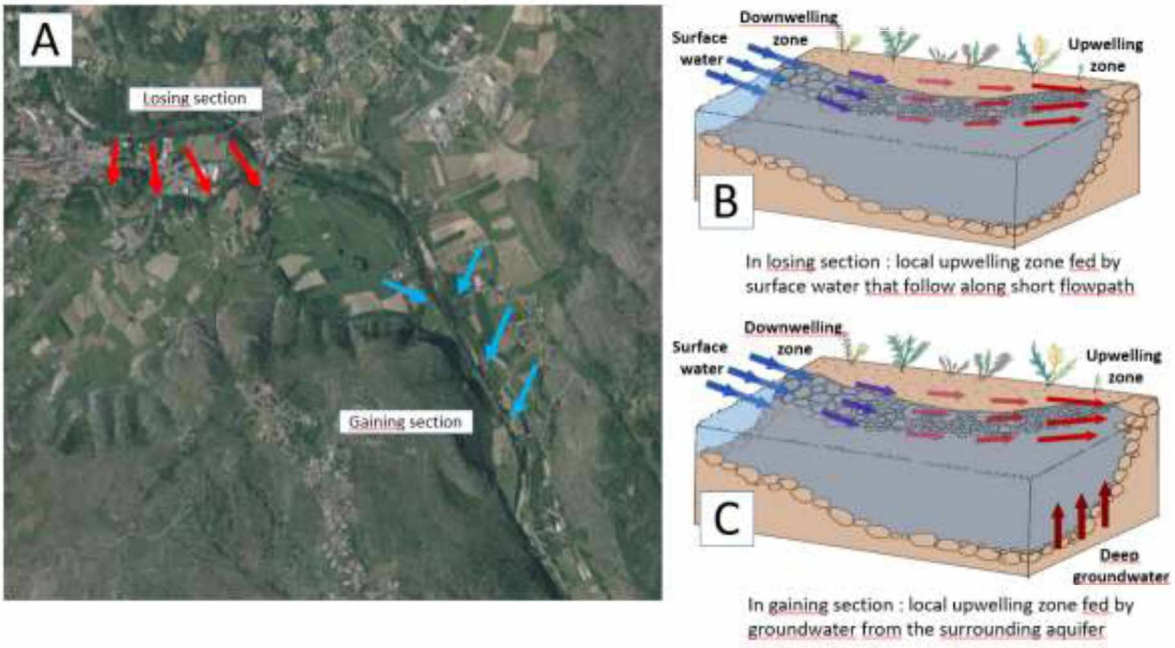

Fig. S1 : Interaction between processes controlling exchanges between river and groundwater. At the section scale (km), losing and gaining sections are controled by the geographical and geological characteristics of the river (A, the Baume River, France). At the local scale, irregularities in the river slope (e.g. riffle, gravel bars, logs…) induce local downwellings followed by local upwellings. In a losing context (B) the chemical characteristics of the upwelling water are similar to surface water, while in a gaining section (C) water chemistry shows influence of deep groundwater.

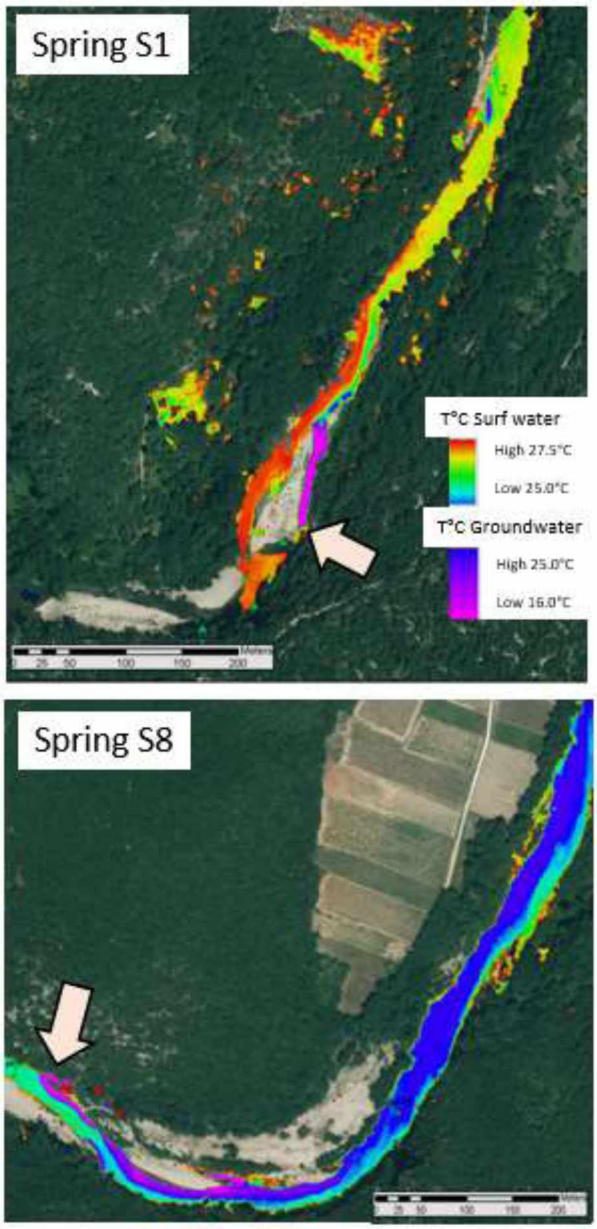

804

805 Figure S2. Aerial infra-red photographs of two sections of the Cèze River close to the Spring S1 (kp 5)

806 and the S8 spring (kp 17) with cold water plumes in blue-violet colours (between 16 and 25°C)

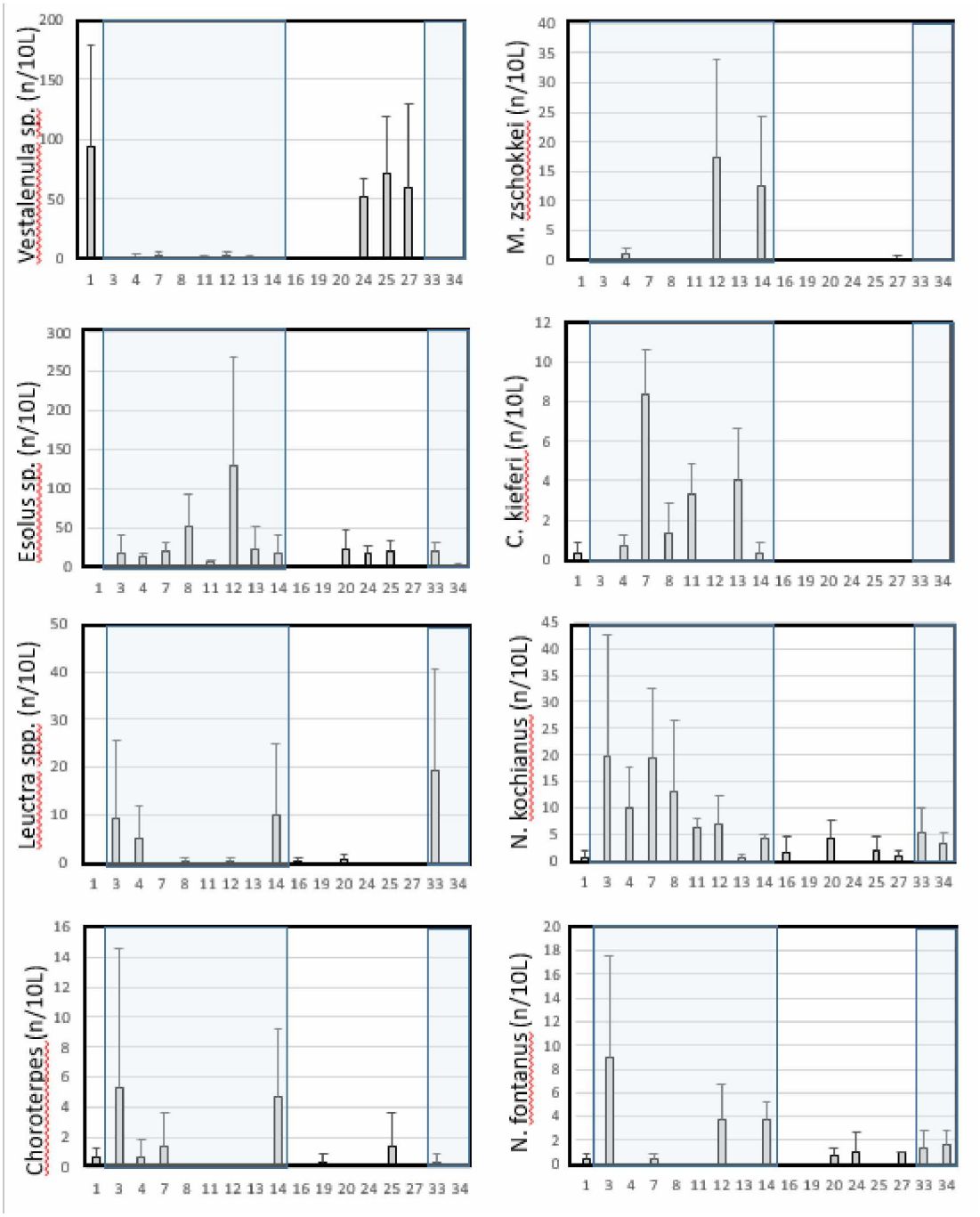

Figure S3: longitudinal distribution of 8 hyporheic organisms of the Cèze River with limits of the gaining sections (blue area, obtained using ^{222}Rn concentrations). The ostracods *Vestanlenula* sp. and *Marmocandona zschokkei*, *Cryptocandona kieferi*, the Coleoptera *Esolus* sp., the Plecoptera *Leuctra* ssp. (sum of *L. major* and *L.* gr *nigra*), the Ephemeroptera *Choroterpes picteti* and the Amphipods *Niphargus kochianus* and *N. fontanus*.